

The Influence of Mass Loading on Particle Distribution in the Near Field of a Co-Annular Jet

C.H. Birzer^{1,2}, P.A.M. Kalt¹, G.J. Nathan¹ and N.L. Smith²

¹School of Mechanical Engineering
The University of Adelaide, SA, 5005 AUSTRALIA

²School of Chemical Engineering
The University of Adelaide, SA, 5005 AUSTRALIA

Abstract

The effects of mass loading on the distribution of spherical particles in the near field of a co-annular jet have been investigated using planar laser light nephelometry. Particle concentrations were measured for nine different mass loading ratios ranging from $\phi = 0.19$ to 1.88, in the first 15 nozzle diameters downstream. Results indicate that particle mass loading has a significant effect on the near field region. The length of the initial triangular core region of approximately uniform particle distributions varies by more than a factor of two, as does its shape. The mass loading ratio also influences the centreline particle concentration decay rates. The effects of mass loading on the signal attenuation are also assessed.

Introduction

Two-phase co-annular jets are widely used, for example to mix fuel and air in pulverised fuel combustion systems. The distribution of particles in the emerging jet stream plays a controlling influence on their subsequent combustion performance. However only limited data are available of particle distributions in such systems. Data for single phase co-annular jets exist [1], however the presence of particles can have a pronounced effect on the structure of the underlying gas flow field [2]. Furthering the understanding of the particle distribution will enable improvements into the combustion of co-annular pulverised fuel systems.

The mass loading ratio, ϕ , is defined as the ratio of solid phase mass flow rate to gas phase mass flow rate,

$$\phi = \frac{m_p}{m_f} \quad (1)$$

where subscripts p and f designate particle and fluid respectively.

Di Giacinto *et al.* [3] investigated the effect of ϕ on velocity and pressure by a simulation of a pressure metering device. These results highlight the coupling between particles and fluid. Fan *et al.* [4, 5] used a Laser Diffraction Method (LDM) to measure particle concentration in the fully merged, self-similar region of co-annular jet flows, 10 to 30 nozzle diameters downstream. Their work comprised three different values of mass loadings for different velocities of the central jet (and therefore particles) and of particle diameters. They found that the fully merged zone for a two-phase turbulent co-axial jet exhibits self similarity in particle concentration and that the rate of particle dispersion is decreased with an increase in particle loading. Black *et al.* [6] used phase Doppler particle anemometry (PDPA) to measure the velocity of spherical and non-spherical particles emerging from co-axial and swirling flows. Their results pertain specifically to velocity. However, they highlighted that particle momentum in the region immediately downstream from the jet plays a significant role in

velocity variations between gas, spherical and non-spherical particles.

To the authors knowledge no published results exist which isolate the influences of solid particle mass loading and particle momentum on the particle distribution in the near field of a co-annular jet. The near field has particular importance in the stabilisation of pulverised fuel flames.

Previous measurements of particle concentration have been obtained from particle counting. Planar nephelometry (a method of measuring concentration based on scattered light) does not appear to have been used for measuring particle distributions in jet flows before, probably because they are subject to errors associated with attenuation of the incident and scattered light beams. Where they are viable, however, planar imaging techniques have the advantage of providing additional information of the instantaneous flow structures, such as regions of local and/or temporal preferential concentration. These issues can not be successfully identified from single point techniques. The effects of particle mass loading on attenuation is therefore of interest, but has also yet to be assessed. The current work provides preliminary data to determine the extent of attenuation for different mass loading ratios.

Background

Particles suspended in a flow will respond to, and cause disturbances in, the suspending flow. Analysis of the motion of particles in a fluid can be based on the inertia of a particle, using the Stokes number, [7], particle dispersion, using the turbulent Schmidt number [5] and the mass loading ratio [3].

The Stokes number is defined as the ratio of particle relaxation time, τ_p to fluidic time scale, τ_f [8]

$$St = \frac{\tau_p}{\tau_f} \quad (2)$$

Used to predict how individual particles respond to the localised fluid flow, the Stokes number neglects the influence of surrounding particle induced fluid perturbations.

The turbulent Schmidt is defined as,

$$Sc_p = \frac{\nu_t}{\epsilon_p} \quad (3)$$

where ν_t is the effective turbulent kinematic viscosity of the gas and ϵ_p is the diffusivity of the particles due to turbulence. Fan *et al.* [5] determined that the influence of mass loading was minimal. They calculated that the turbulent Schmidt number varies only between 1.4 and 1.5 with changes in mass loading over the range of 0.5 to 1.5.

To avoid the above complications, the present investigation into the effects of mass loading on particle dispersion is conducted with fixed values of Stokes number. Instantaneous planar concentration measurements of the particle distribution from the central jet of a co-annular nozzle were recorded for a range of mass loadings up to 17 diameters downstream.

Equipment

Experiments were conducted in a purpose built open loop wind tunnel with 650mm x 650mm square cross section as shown in figure 1. It is vertically down fired to avoid any bias due to gravity. A bell-mouth inlet and flow conditioning screens (not shown) were used to provide a co-flow with steady and uniform velocity of approximately 8m/s.

Q-Cel™ hollow glass spheres with a particles diameters range from 25-45 microns with a density of approximately 700kg/m³ were introduced into the central jet via a fluidised bed feeder. Mass loadings were determined by the change in mass of the feeder, as measured by a load cell and fulcrum and recorded on a computer. Calibration of the feeder was conducted before and after each experimental run.

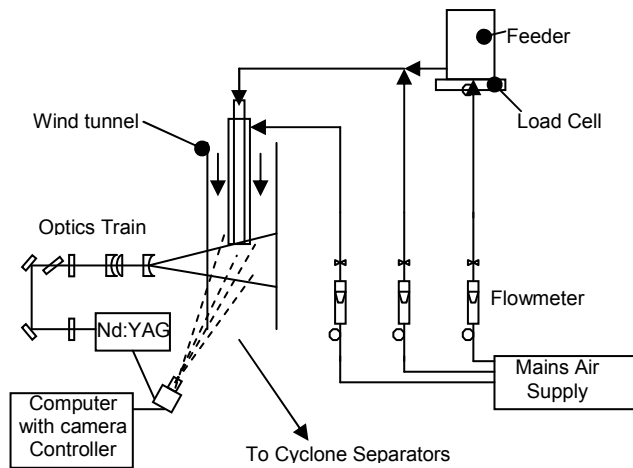


Figure 1. A schematic representation of the experimental layout.

Controlling of the particle mass flow rate was achieved by varying the amount of fluidising air as measured by a Fisher & Porter FP ¼-10-SS flow meter. The resulting variation of total air flow through the central jet was measured to be ±0.5m/s, which equates to less than a 2% error.

The nozzle and dimensions are shown in figure 2. The development length of the central and annular nozzles is in excess of 100 diameters to avoid bias and allow fully developed initial flow. Constant flow velocities of $U_1=42\text{m/s}$ and $U_2=73\text{m/s}$ were obtained using FP ½-27-G-10/83 with GSVT 44 float and FP-1-27-G-10/83 with a GSVT 64 float. The fluid based momentum ratio (G_1/G_2) for the configuration is 0.115. The addition of particles results in a momentum ratio ranging from 0.116 to 0.118. Tabulated data are given in table 1.

A frequency doubled Nd:YAG laser, pulsed at 10Hz was used to produce a light sheet approximately 3mm thick through the central plane of the jet. Light scattering was recorded on a Kodak Megaplus Class 1 CCD, with exposure time of 6.487 msec and trigger by the laser flashlamp. Each experiment yielded 448 images with 10 bit resolution.

Technique

Instantaneous planar concentration measurements were conducted using planar nephelometry. As the particles are much larger than the laser beam wavelength the Mie scattering theory, as outlined by Becker [9] may not apply. The CCD was aligned at 90 degrees to the incident beam to minimise image distortion. Variations in laser sheet intensity have been accounted for by using a mean image of the laser sheet profile, obtained by filling the tunnel with smoke (with the fan not operating).

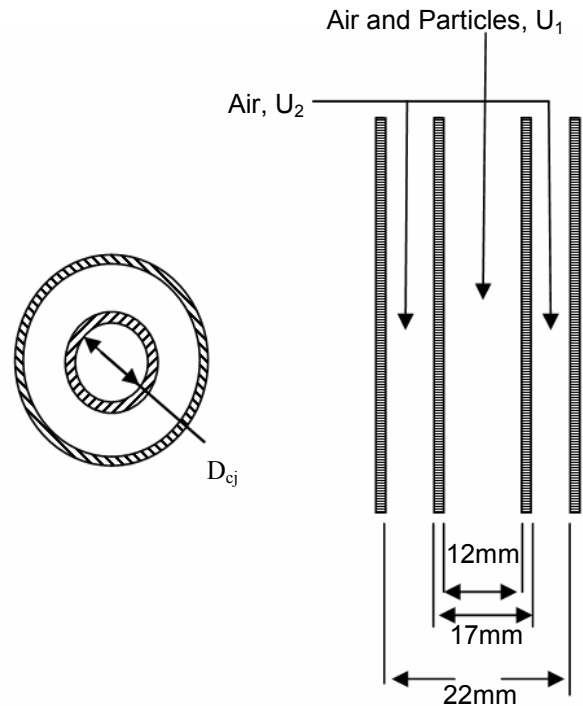


Figure 2. The nozzle design.

Results and Discussion

Centreline Distribution / Decay Rates

Figure 3 presents a set of mean particle distribution images for a range of mass loading ratios. A colour map has been used for clarity.

The higher momentum of the annular jet, relative to the central jet, results in a necking of the flow so that the region of maximum particle concentration is located not at the nozzle exit, but some distance downstream. Figure 4 plots the centreline particle concentration normalised to the maximum concentration for each mass loading ratio. There is a distinct difference between centreline particle decay rates for varying mass loading ratios. Fan *et al.*[5] showed that the higher mass loading cases had a reduction in jet spread, which complements a lower decay rate. The effect of mass loading on the axial location of the peak concentration is presented in figure 5. It can be seen that increasing the mass loading by an order of magnitude causes the location of the maximum concentration to move downstream by almost two nozzle diameters. Mean images shown in figure 3 indicate that the overall shape of the potential core is also elongated by an increase in mass loading. The increase in mass loading ratio equates to an increase of less than 0.5% to the central jet momentum. Particle inertia may have an influence on near field structure, however the current data has isolated mass loading from individual particle inertia.

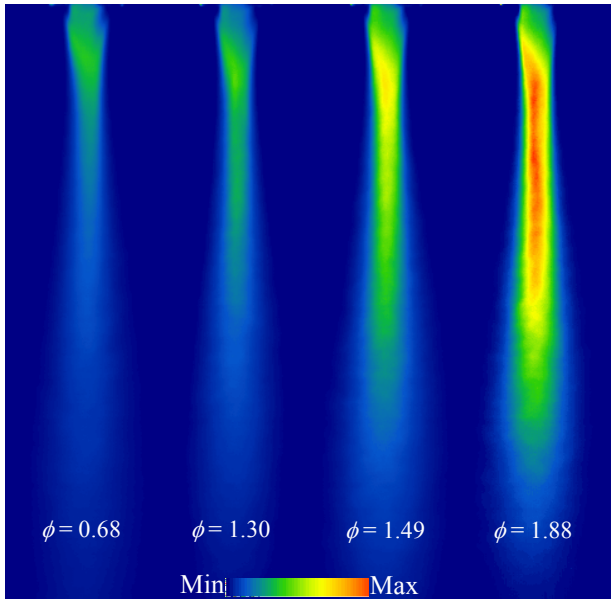


Figure 3. A set of images of the mean particle distributions for, from left to right, $\phi = 0.68, 1.30, 1.49, 1.88$. Colour map used to highlight variation in particle concentration.

It is expected that that the virtual origin of the jet also depends on the change in mass loading. However, the current data is limited to 15 nozzle diameters downstream so that reliable measurements of the virtual origin cannot be obtained.

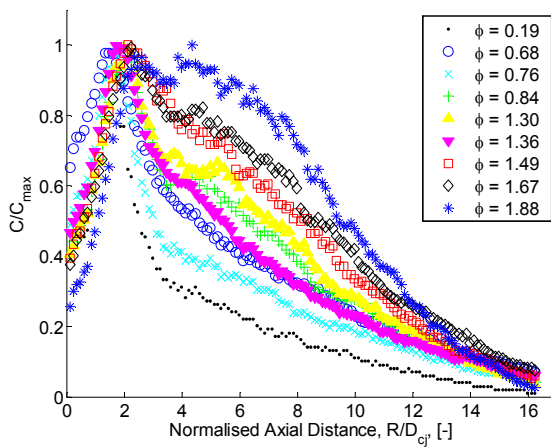


Figure 4. Centreline concentration profiles for all mass loading ratios normalised to the maximum concentration.

Radial Profiles

Figure 6 shows a series of radial profiles for the $\phi = 1.30$ case. The concentration has been normalised to the maximum radial concentration. Radial distances (R/D_{c_j}) have been normalised by the axial distance from the nozzle, x/D_{c_j} , in the absence of an accurate measurement of the location of the virtual origin. Here R is the radial distance from the centre of the jet, D_{c_j} is the inside diameter of the central jet and x is the axial distance downstream.

Further downstream, the radial profiles collapse to be self similar. The current findings indicate that the location at which mean similarity begins is approximately 5 diameters from the nozzle. Previous findings [5] only detailed radial profiles between $x/D_{c_j} = 10$ to 30.

At $x/D_{c_j} = 1$ the radial concentration is expected to follow a top-hat profile. The effect of attenuation to the incident beam can be

clearly seen by the asymmetrical concentration with respect to the incident laser sheet as discussed in Errors

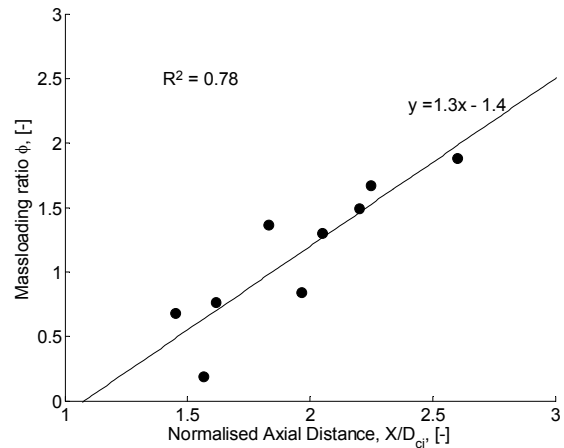


Figure 5. Location of the maximum centreline concentration peak for all mass loading ratios normalised to the exit concentration.

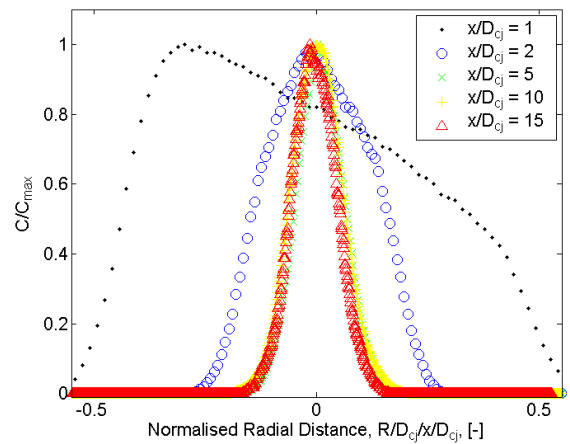


Figure 6. Radial profiles for the case of $\phi = 1.30$.

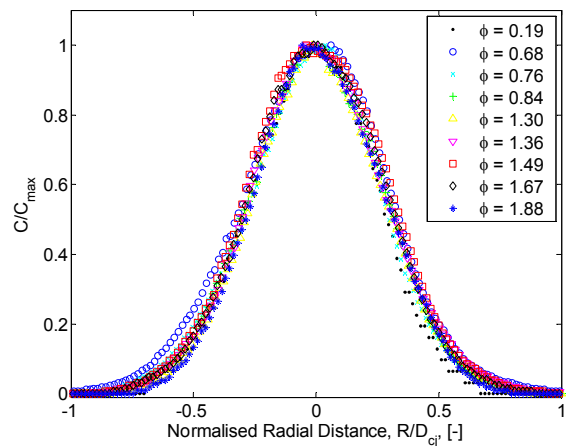


Figure 7. Radial profiles at $x/D_{c_j} = 5$ for varying mass loading ratios.

The radial profiles of the 9 mass loading ratios at $x/D_{c_j} = 5$ are shown in figure 7. Concentration is normalised to the maximum concentration and the radial distance is normalised to the central jet inside diameter. The radial profiles of all mass loadings at $x/D_{c_j} = 10$ and 15 also appear to collapse. However, this does not necessarily contradict the finding of Fan *et al.* [5] that spreading rate decreases with mass loading. Since the location of the virtual origin also shifts with mass loading, the similarity of spread any given axial location cannot be considered in isolation.

Errors

It is argued that the largest source of error is from attenuation of light which can be seen indirectly the near nozzle regions in figure 3. An increase in mass loading causes an increase in particle volume fraction and surface area, attenuating both the laser beam and the scattered signal.

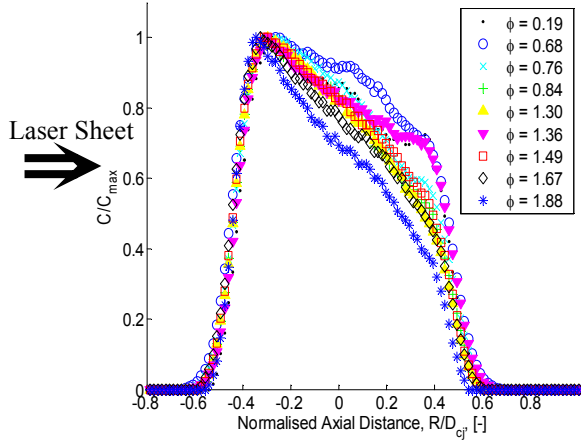


Figure 8. Radial profiles at $x/D_{cj} = 1$ indicating the attenuation.

Figure 8 presents radial profiles at $x/D_{cj} = 1$ for the 9 cases. In this region particle concentration is high and therefore any effects of attenuation are severe. Uniform particle concentration and no effects of attenuation would be represented by symmetry about the centreline. A reduction in normalised concentration can be seen from left to right of the graph, the direction the beam travels. The general trend is that lower mass loadings have a lower absolute rate of change of the normalised concentration. If the above mentioned effect was a result of biased particle concentration then the rate of change in normalised concentration of the different loading cases would be similar. Any major bias of particle concentration would also be prominent further downstream, where attenuation effects are reduced by particle dispersion. It can be seen in figure 6, that bias downstream is not significant. Furthermore, during the experimentation, no bias in particle concentration was seen visually.

	Flow Conditions	
	Fan <i>et al.</i> [5]	Current work
Particle Diameter	70 microns	25 - 45 microns
Particle Density	1250 kg/m ³	700 kg/m ³
Stokes Number	77	37
Central Jet Diameter	40mm	12mm
Annular Jet Diameter	68mm	20mm
Central Jet Velocity	20 m/s	42 m/s
Central Jet Reynolds Number	52,000	28,000
Annular Jet Velocity	30 m/s	73 m/s
Annular Jet Reynolds Number	134,000	110,000

Table 1. Particle and flow data of current work and that of Fan *et al.* [5].

Conclusions

The effects of particle mass loading on particle concentration in co-annular jets have been assessed. Planar nephelometry was used to investigate mass loading ratios ranging from $\phi = 0.19$ - 1.88 at fixed fluid velocities and particle Stokes numbers. Data of the first 15 nozzle diameters downstream have yielded the following observations:

- 1) A necking region occurs downstream from the nozzle exit where the particle concentration increases significantly above the exit value.
- 2) The length of the “potential core” region of uniform concentration increases by almost two diameters with an order of magnitude increase in mass loading.
- 3) The mean rate of centreline particle concentration decreases with increase mass loading.
- 4) The mean radial profiles are approximately self similar beyond $x/D = 5$ for each mass loading investigated.
- 5) For the present particles, the effects of attenuation on measurement accuracy are diminished beyond $x/D_{cj} = 2$.

Acknowledgments

The authors acknowledge the financial assistance provided to this project by the Australian Research Council through its large grant scheme.

The authors also thank Mr Grant England, Miss Sarah Crook and Mr Billy Constantine of the School of Mechanical Engineering, The University of Adelaide, Adelaide, for the assistance with data collection and analysis.

References

- [1] Wall, T.F., Nguyen, H., Subramanian, V., Mai-Viet, T. and Howley, P., Direct Measurements of the Entrainment by Single and Double Concentric Jets in the Regions of Transition and Flow Establishment, *Trans. IChemE*, **58**, 1980, 237-241.
- [2] Fan, J., Zhang, X., Chen, L. and Cen, K., New Stochastic Particle Dispersion Modeling of a Turbulent Particle-Laden Round Jet, *Chem. Eng. J.*, **66**, 1997, 207-215.
- [3] Di Giacinto, M., Sabetta, F., and Piva, R., Two-Way Coupling Effects in Dilute Gas-Particle Flows, *J. of Fluids Eng.* **104**, 1982, 304-312.
- [4] Fan, J., Zhao, H. and Cen, K., An Experimental Study of Two-Phase Turbulent Coaxial Jets, *Exp. Fluids*, **13**, 1992, 279-287
- [5] Fan, J., Zhao, H. and Cen, K., Particle Concentration and Size Measurements in Two-Phase Turbulent Coaxial Jets, *Chem. Eng. Comm*, **156**, 1996, 115-129.
- [6] Black, D.L., and McQuay, M.Q., Laser-based Particle Measurements of Spherical and Nonspherical Particles, *Int. J. Multiphase Flow*, **27**, 2001, 1333-1362
- [7] Aggarwal, S., Relationship between Stokes Number and Intrinsic Frequencies in Particle-Laden Flows, *AIAA J.*, **32**, 1993, 1322-1324.
- [8] Kulick, J.D., Fessler, J.R., and Eaton, J.K., On the Interactions between Particles and Turbulence in a Fully-Developed Channel Flow in Air, *Internal Report Stanford University, Stanford, California, MD-66*, 1993.
- [9] Becker, H.A. Mixing, Concentration Fluctuations, and Marker Nephelometry, in *Studies in Convection, Vol 2. Theory, Measurements and Applications*, editor, Launder, B.E., Academic Press, 1977, 45-139.